2016 IEEE/RSJ International Conference on Intelligent Robots and Systems (IROS)
Daejeon Convention Center
October 9-14, 2016, Daejeon, Korea

Robust Impedance Control with Applications to a Series-Elastic Actuated System

Kevin Haninger, Junkai Lu and Masayoshi Tomizuka

Abstract— **Impedance control offers a theoretical basis for safe interaction between a robot and the environment, but model uncertainty, disturbances and actuation dynamics can compromise the accuracy of the rendered impedance in implementation. If both the interactive force and motion are directly sensed, the relationship between them can be robustly regulated to present the desired impedance dynamics. In this paper, a Disturbance Observer based controller architecture is presented which offers performance robustness for impedance control. Conditions for stability and passivity are developed, then this controller is analyzed on a series-elastic actuated system. The effect of actuation dynamics on both performance and stability is analyzed, then experimental results are presented.**

I. Introduction

Traditional controllers track a system output as closely as possible, rejecting disturbances or perturbations to track desired output. For interactive robots, some external forces come from the environment, and it is more useful to regulate the relationship between external force and position, rather than either one independently [1], [2]. Typically, either force or motion is taken as exogeneous input (for admittance or impedance control respectively [3]), and the other quantity is controlled to respond according to the desired dynamics, the impedance.

Although the theory is elegant, several real-world considerations can be important. The issues discussed here stem from the dynamics between the interaction port (where the desired impedance is to be achieved) and the actuator which drives these quantities. Seen in Figure 1 is a linear second-order system, driven by actuator and interactive torques. This basic model will be used to introduce several challenges and corresponding approaches which have been explored in impedance control research.

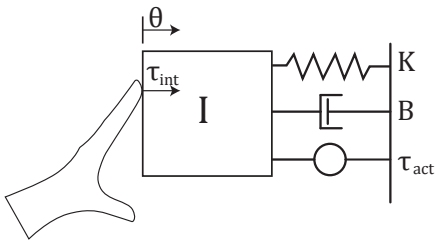

Fig. 1. Interactive system model, with actuator

This work supported by NSF EFRI Grant #1137267
Authors affiliated with Department of Mechanical Engineering, University of California, Berkeley, CA 94720 USA (e-mail: {khaninger, junkai.lu, tomizuka}@berkeley.edu)

One fundamental challenge for impedance control is that actuators have dynamics of their own, i.e. are not ideal force sources. Although in some cases a backdriveable actuator can be used directly [4], commercially available actuators often require significant gear reduction to meet the required torque specifications. A gearbox or drivetrain introduces additional dynamics, especially when backdriven by the environment. One option is to integrate a torque sensor after the gearbox, allowing an inner-loop torque controller which reduces the apparent dynamics of the actuator [5]. The integration of a torque sensor increases complexity and cost, but may offer good performance. A related approach is series elastic actuators (SEAs), which insert a spring in the drivetrain and measure torque by the displacement on the spring [6], [7], [8], [9], [10]. This torque measurement can then be used in an inner-loop torque control, and the physical compliance offers lower impedance at high frequencies (beyond the bandwidth of the torque controller). Although less expensive, an SEA design is mechanically complex, and the significant higher-order dynamics introduced by the relatively low stiffness spring can make controller design challenging.

Typically joint torque controlled robots are used for impedance control, where position error and desired impedance determine the force command for the inner-loop torque control. The torque sensor located after the actuator helps address the actuator dynamics and significantly improves interactive performance. However, note that in these hardware approaches, interaction force is not directly sensed, but inferred from measurements closer to the actuator, with some dynamic elements between the interaction port and sensor.

As the actuator torques are not directly applied to the environment, but pass through kinematic structure to the interaction port, another challenge is the dynamics of the interactive device itself. Many of the early mechanical devices for interactive control are designed to be lightweight and low friction [15], [16]. In such a system, the mechanical system's dynamics can be neglected and the impedance directly realized on the actuators. However, higher load or higher DOF applications of interactive robots may require a mechanical system which has significant, difficult to model dynamics.

Any unmodelled dynamics or disturbances between the torque-controlled element and interaction port will directly affect the rendered impedance, as they are not distinguished from the interaction force. By increasing the response to external force, the response to (for example) unmodelled coulomb friction is increased.

978-1-5090-3762-9/16/$31.00 ©2016 IEEE

Another approach, admittance control, addresses actuator backdriveability and system dynamics together by including a force/torque sensor directly at points of interaction. These force/torque measurements, combined with the desired admittance, define desired motion for an inner-loop motion controller. Established position control techniques can achieve good robustness in tracking the desired trajectory [11], [12], [13], [14]. However, above the bandwidth of the position controller, the system's (high impedance) dynamics cannot be modified to present a desired behavior.

By using more advanced controller design techniques, some have improved the performance of feedback impedance control [17], [18], [19], [20]. Others have used the Disturbance Observer (DOB) to estimate the interactive force indirectly by using a nominal model, then use this estimate in a feedback law [22], [23]. Others have used the DOB to enforce model dynamics of the robot in a force or impedance control task [24], [25].

This paper introduces a disturbance observer based approach which regulates the interactive closed-loop dynamics to that of the desired impedance. Just as traditional feedback control must directly measure an output to robustly regulate it, this approach uses direct measurement of both interactive force and motion to robustly achieve the desired relationship between them (i.e. the desired impedance). This approach is most similar to that used in [26], [18], where the 'dynamic error' (i.e. $\tau_{int} - G_{imp}\theta$, where G_{imp} is desired dynamics and $\{\tau_{int}, \theta\}$ desired port variables to regulate) is corrected with feedback. However, here the DOB is used to regulate this dynamic error, which allows rigorous treatment of multiplicative uncertainty and a simple tuning methodology. First, a linear system is used to introduce conventional impedance control and the DOB approach. Sufficient conditions for the stability and passivity of the DOB approach are developed. Then, the effects of implementing this approach on a series-elastic actuator system are studied. Finally, experimental results validate these analyses.

II. Model Based Controller Design

This section introduces classical impedance control and analyzes the effect of model uncertainty and disturbances on the impedance rendered at the interactive port. Let the system in Figure 1 be described by

$$I\ddot{\theta} + B\dot{\theta} + K\theta = \tau_{int} + \tau_{act} \tag{1}$$

where I, B and K are the true inertia, damping and stiffness respectively. The system is driven by actuator and interactive torques τ_{act} and τ_{int}, and achieves position θ. Suppose a dynamic model of the robot, with corresponding nominal values $\hat{I}$, $\hat{B}$, and $\hat{K}$. A controller can use this model to compensate the robot's dynamics in realizing a desired impedance, such as:

$$\tau_{act} = \left(\hat{I} - I_{imp}\right)\ddot{\theta} + \left(\hat{B} - B_{imp}\right)\dot{\theta} + \left(\hat{K} - K_{imp}\right)\theta \tag{2}$$

where τ_{act} is the actuator force, and $[\cdot]_{imp}$ denotes the desired impedance parameters. Typically, the impedance mass will be taken to be the model system mass, as $\ddot{\theta}$ is usually inferred from position sensors and will be noisy, although some have explored changing the apparent mass [27].

A. Inverse Dynamic Compensation

A block diagram realization of (2) is shown in Figure 2, generalized to a linear plant $G(s) = (Is^2 + Bs + K)^{-1}$, corresponding nominal model $\hat{G}(s)$ and desired impedance $G_{imp}(s) = I_{imp}s^2 + B_{imp}s + K_{imp}$. The inputs τ_{int}, τ_{act} and d are the interactive, actuator and disturbance torques respectively.

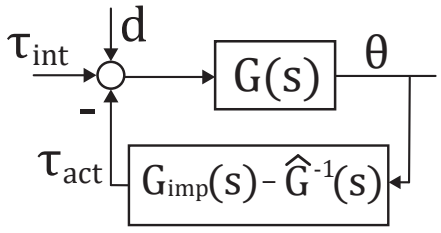

Fig. 2. Inverse dynamic compensation for impedance control

Any disturbance will cause a position response the same as τ_{int}, as the two are not distinguished by the controller in this approach.

B. Stability of Inverse Dynamic Compensation

The stability of the block diagram shown in Figure 2 will be investigated in this section under the assumption that relations between the true dynamics, model, and desired impedance are

$$G(s) = \hat{G}(s)(1 + \Delta(s)) \tag{3}$$

$$G_{imp}(s) = \hat{G}^{-1}(s)(1 + \Omega(s)) \tag{4}$$

where $\Delta(s)$ characterizes the model uncertainty, and has a bounded, known magnitude. The quantity $\Omega(s)$ characterizes the difference between the nominal model and the desired impedance, and is known. This gives a closed-loop transfer function from τ_{int} to θ of

$$G_{idc} = G_{imp}^{-1}\frac{1 + \Delta}{1 + \Delta\Omega(1 + \Omega)^{-1}}. \tag{5}$$

For $\|\Delta(s)\| \neq 0$, this system diverges from the desired transfer function G_{imp}^{-1}. The stability of (5) can be shown by using the small gain theorem. Sufficiency for stability is G be stable, $(1 + \Omega)$ be minimum-phase stable and

$$\left\|\frac{\Delta(j\omega)\Omega(j\omega)}{1 + \Omega(j\omega)}\right\| < 1 \qquad \forall\omega. \tag{6}$$

Typically this (conservative) condition will not be difficult to meet, but other aspects of an implementation may compromise stability. Early studies examined interaction port behavior and Lyapunov stability [28], while others have considered impedance control stability under time delay [29] and discretization [27].

III. Robust Impedance Control

In the controllers above, performance was limited by model accuracy and the presence of disturbances. This section will present an approach which can use direct measurement of $\{\theta, \tau_{int}\}$ to enforce the desired impedance.

A. Disturbance Observer

The disturbance observer is a practical tool to improve performance in feedback control systems [30]. In a traditional DOB, an inverse model of the plant and observed output are used to estimate disturbances and enforce that the closed-loop system has the model dynamics.

If in the feedback path of the DOB the impedance dynamics are used instead of the inverse plant dynamics, the DOB will enforce the desired impedance dynamics. The proposed architecture is shown in Figure 3, where $Q(s)$ is a low-pass filter introduced to allow tuning and make $G_{imp}(s)Q(s)$ realizable.

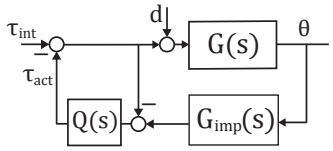

Fig. 3. Disturbance observer based impedance control

In this architecture, the expression for θ is

$$\theta(s) = \frac{G}{1+QGG_{imp}-Q}\tau_{int}(s) + \frac{G(1-Q)}{1+QGG_{imp}-Q}D(s) \tag{7}$$

When $Q(s) = 1$, the transfer function from τ_{int} to θ approaches the desired transfer function G_{imp}^{-1}. Also, the transfer function from D to θ goes to 0, giving ideal disturbance rejection.

The θ which is put in feedback can be regarded as the deviation from a desired position to achieve trajectory tracking.

1) Stability of DOB Impedance Control: As stability of a DOB is limited by the difference between the inverse model and the actual system dynamics, the block diagram in Figure 4 is introduced. The $G_{imp} - \hat{G}^{-1}$ term compensates known discrepancies between the model and desired impedance, and the DOB loop robustly enforces the desired impedance.

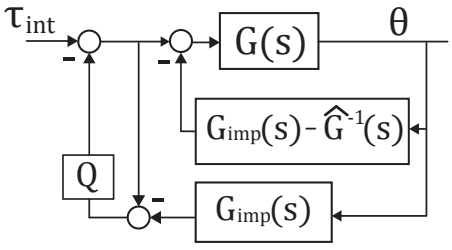

Fig. 4. Inner loop compensation DOB

Note that the term $G_{imp} - \hat{G}^{-1}$ is not in general realizable. Typical implementations of impedance control only change the damping and stiffness of the system, so this term will usually take the form $\tilde{B}s + \tilde{K}$, and can be realized with differentiation of θ.

This block diagram structure gives a closed-loop transfer function from τ_{int} to θ of

$$G_{dob} = \frac{G}{1-Q+G_{imp}G-(1-Q)G\hat{G}^{-1}}. \tag{8}$$

Again, using the multiplicative uncertainty models in (3) and (4) allows stability analysis. A sufficient condition for stability requires G should be stable, $(1+\Omega)$ minimum-phase stable and

$$\left\| \frac{\Delta(j\omega)(\Omega(j\omega)+Q(j\omega))}{1+\Omega(j\omega)} \right\| < 1 \qquad \forall\omega. \tag{9}$$

The disturbance rejection properties are preserved with the inner-loop compensation, and can be shown with a similar approach to that shown in (7).

In the block diagram proposed in Figure 4, the control action takes the form

$$\tau_{act} = \frac{Q}{1-Q}(\tau_{int} - G_{imp}\theta) - \left(G_{imp} - \hat{G}^{-1}\right)\theta. \tag{10}$$

2) Passivity of DOB Impedance Control: Passivity of the controlled system allows stability to be concluded when the system is coupled with any passive environment [1]. In the proposed approach, if the model uncertainty goes to zero ($\Delta \to 0$), passivity can be immediately found from passivity of $G_{imp}(s)$. However, Δ is a magnitude-bounded uncertainty (i.e. unknown phase) and passivity (for linear systems, positive realness) is a phase condition. The Cayley Transform can be used, where if T is positive real, $\|(T-1)(T+1)^{-1}\| < 1$ [31]. Applying this transform here to $sG_{dob}(s)$ with the $\mathcal{H}_\infty$ norm gives

$$\left\| \frac{\hat{G}(s+G_{imp})+\tilde{\Delta}}{\hat{G}(s-G_{imp})-\tilde{\Delta}} \right\|_\infty < 1, \tag{11}$$

where $\tilde{\Delta} = (1-Q)\Delta(1+\Delta)^{-1}$. A sufficient condition for this constraint on a SISO system is

$$\left|\hat{G}(j\omega+G_{imp})\right| + 2\left|\tilde{\Delta}\right| < \left|\hat{G}(j\omega-G_{imp})\right| \quad \forall\omega. \tag{12}$$

Note that the tuning filter Q appears in both (12) and (9), and can be selected to meet both these frequency domain criteria.

IV. Series-Elastic Actuated System

Here, the effect of actuation dynamics on the DOB controller will be investigated on a series-elastic actuated system [8], [9], [32]. Let the SEA, integrated to an inertial system, be as shown in Figure 5, where J is the motor inertia viewed from the output of the gearbox, I is the load-side inertia, ϕ and θ are their respective positions, and K_{sp} is the stiffness of the spring which couples them. Motor torque and interactive

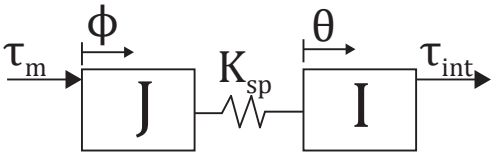

Fig. 5. Series-elastic actuator integrated to driven inertia

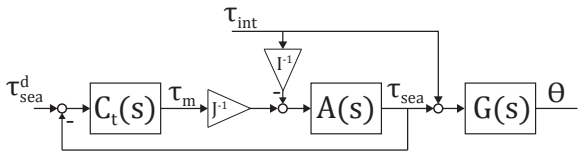

Fig. 6. Inner-loop torque-mode control

torque, τ_m and τ_{int}, drive the system. Under the proposed model,

$$K_{sp}^{-1}\ddot{\tau}_{sea} = -\left(I^{-1}+J^{-1}\right)\tau_{sea}+\tau_m J^{-1}-\tau_{int}I^{-1} \quad (13)$$

where $\tau_{sea} = K_{sp}(\phi-\theta)$.

A. Torque-mode Control

This model under closed-loop torque control with control law $\tau_m = C_t(s)\left(\tau_{sea}^d - \tau_{sea}\right)$ is shown in Figure 6, where $A(s)$ is defined as

$$A(s) = \frac{1}{K_{sp}^{-1}s^2+\left(I^{-1}+J^{-1}\right)}. \quad (14)$$

The closed-loop dynamics can be found as

$$A_{cl}(s) = \frac{\tau_{sea}}{\tau_{sea}^d} = \frac{C_t(s)A(s)}{J+C_t(s)A(s)} \quad (15)$$

$$A_{int}(s) = \frac{\tau_{sea}}{\tau_{int}} = \frac{JA(s)}{IJ+IC_t(s)A(s)}. \quad (16)$$

B. DOB with Actuator Dynamics

The system with actuator dynamics under DOB control can be seen in Figure 7. The DOB outer-loop is realized as in (10), with $\tau_{act} = \tau_{sea}^d$. Writing the expression from τ_{int} to θ under the controller shown in Figure 7

$$\frac{\theta}{\tau_{int}} = \frac{GA_{cl}Q+(1-Q)G(1+A_{int})}{1-Q+GA_{cl}G_{imp}-(1-Q)GA_{cl}\hat{G}^{-1}}. \quad (17)$$

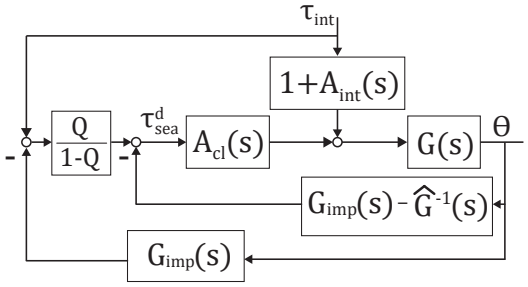

Fig. 7. Integrated inner loop control with DOB

When $Q(s) = 1$, the desired dynamics are recovered, so performance robustness with an uncertain G can be preserved even with actuator dynamics. In practice, the addition of actuator dynamics will reduce the maximum $\|Q\|$ which can be safely realized, reducing performance of the DOB approach compared with an ideal force source.

1) Stability with Actuation Dynamics: Looking at the denominator of (17), and taking the same multiplicative uncertainty model shown in (3) and (4), a sufficient stability criteria can be found. If G, A_{cl} and A_{int} are stable, the following condition must also be met at all frequencies:

$$\|A_{cl}\|\left\|-QA_{cl}^{-1}+(\Omega+Q)(1+\Delta)\right\| < 1 \quad (18)$$

Typically, A_{cl} will have unity gain up to some bandwidth (i.e. $\|A_{cl}(j\omega)\| \approx 1,\ \omega \le \omega_c$) and rolling off above that frequency. To keep the term QA_{cl}^{-1} small in the stability criteria, Q could be a low-pass filter with cutoff frequency below that of the actuator.

V. General Dynamic Error Feedback

In some cases, the high-gain control inherent to the DOB is to be avoided. In this case, it is still possible to use direct measurement of interactive force to improve the accuracy of the rendered impedance. In the DOB impedance control, high-gain control corrects the deviation from the desired closed-loop dynamics as

$$\tau_{dob} = \frac{Q}{1-Q}(\tau_{int}-G_{imp}\theta) \quad (19)$$

where τ_{dob} is the component of τ_{act} which can be attributed to the disturbance observer. The expression $\tilde{\tau}_{dyn} = \tau_{int} - G_{imp}\theta$ can be considered as the deviation from the desired impedance dynamics expressed as a force. A position representation of this error is $\tilde{\theta}_{dyn} = G_{imp}^{-1}\tau_{int} - \theta$, which is the basis of admittance control. However, for a system with force as the primitive input (i.e. with direct control over the actuator, instead of an inner-loop position control), this force representation of the dynamic error can be more natural.

This dynamic error term can be compensated with a general compensator $C_{imp}(s)$ to give the following control law:

$$\tau_{act} = C_{imp}(s)(\tau_{int}-G_{imp}\theta)+\left(\hat{G}^{-1}-G_{imp}\right)\theta \quad (20)$$

This then gives the following:

$$\frac{\theta(s)}{\tau_{int}(s)} = G_{imp}^{-1}\frac{C_{imp}N(s)}{1+C_{imp}N(s)} \quad (21)$$

where

$$N(s) = \frac{GG_{imp}}{1-G\left(\hat{G}^{-1}-G_{imp}\right)} \quad (22)$$

This now resembles the classical feedback architecture of a compensator $C_{imp}(s)$ in series with a plant $N(s)$ under negative feedback. Traditional approaches to stability and performance can inform the controller design (e.g. root locus). The design objective of letting τ_{int}/θ approach G_{imp}^{-1} can be achieved by letting $C_{imp}N(1+C_{imp}N)^{-1} \to 1$. This feedback can also be shown to improve the disturbance rejection.

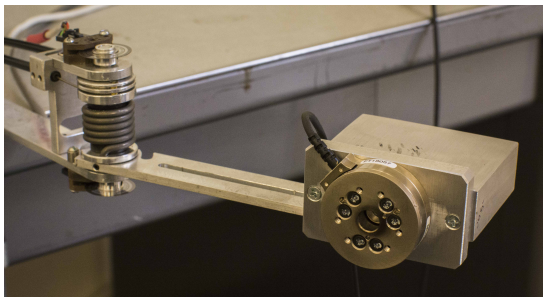

Fig. 8. SEA driven inertia with integrated force sensor

VI. Experimental Validation

The discussed controllers were implemented on a cable-driven series-elastic actuated system for validation. Additional details on the experimental setup can be found in [9]. An ATI Mini45 force/torque sensor was integrated to allow direct measurement of the interactive torque. A picture of the experimental setup can be seen in Figure 8. The DOB implementation used a Q filter of the form

$$Q(s) = \frac{\alpha\omega^2}{s^2 + 1.415\omega s + \omega^2} \tag{23}$$

where $\alpha = .8$ and $\omega = 50$ (rad/sec) were found experimentally. This Q allows compensator realizability (i.e. relative degree of total compensator expression), and has lower magnitude at high frequencies (where model uncertainty increases) to meet the stability condition (9). The dynamic feedback in (20) was realized with $C_{imp}(s) = 2.5$, a lowpass filter on the τ_{int} with cutoff frequency 100 (rad/sec), and first-order differentiation of θ.

First, a quasi-static, manually applied interactive force was slowly increased, then decreased to test the rendering of an almost pure stiffness. The comparison between a traditional controller (2), DOB controller (10), and dynamic feedback (20) can be seen in Figure 9. The effects of coulomb friction on the load side are apparent for all implementations, but greatly reduced under both DOB and dynamic feedback, where dynamic feedback and the DOB have almost identical performance.

Next, a variety of stiffnesses were realized on the DOB system with the same inner-loop and DOB gains. These results are seen in Figure 10. Stiffnesses up to 10 N-m/rad could be realized, which is greater than the stiffness of the SEA spring (4.8 N-m/rad). The low stiffness (.2 N-m/rad) was approaching the limit of stability. Oscillation, possibly from the stick-slip of the bowden cables, is evident in the response. At lower impedances (here, lower stiffnesses), the coulomb friction, which was not fully compensated, is more noticeable in the position response. The second test was performed by exciting the system with a variety of interactive torques for an extended period. Significant frequency content in the interactive torque was in the range 0-50 rad/sec. The frequency domain representation of τ_{int} and θ were used to find the experimental transfer function, shown in Figure 11. The DOB provides a much more accurate rendering of

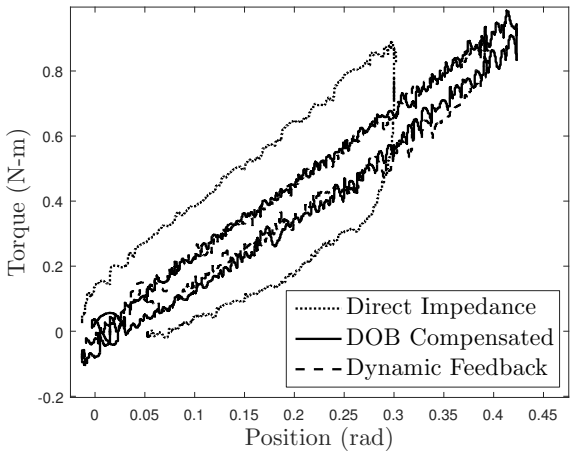

Fig. 9. Stiffness rendering comparison

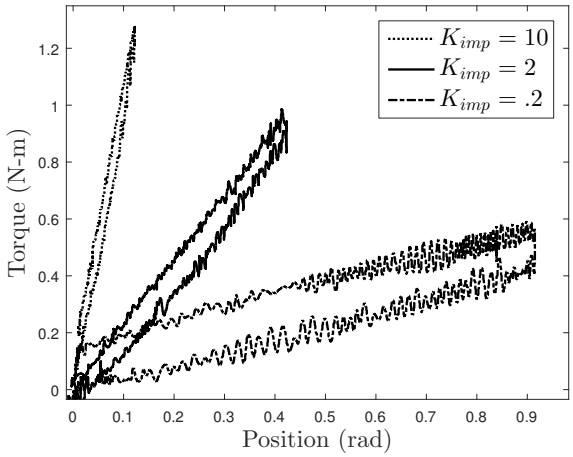

Fig. 10. Variety of stiffnesses rendered with DOB approach

the desired impedance, and the dynamic feedback controller has moderate performance at lower frequencies, but does not match the desired impedance as well at higher frequencies. The performance loss of the traditional controller can be partially attributed to the rather large coulomb friction on the load side of this setup. In Figure 12, the same process was used to render two different impedances on the DOB system ($K_{imp} = 1.25$, $B_{imp} = .35$ and $K_{imp} = 3$ $B_{imp} = .25$ respectively). The DOB system was able to render these two impedances accurately.

VII. Conclusion

The approach proposed in this paper offers an alternative means of realizing interactive control on systems with force sensors and force-mode actuators. It offers performance robustness by direct measurement of the interactive port variables, and lower-frequency performance is maintained even with actuation dynamics. Although similar to admittance control in measuring interactive force, a flexible-joint system offers lower impedance above the controller bandwidth, which may improve performance in high-stiffness environments.

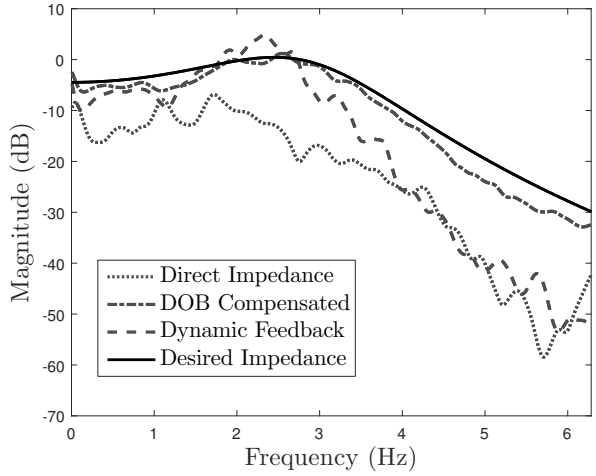

Fig. 11. DOB vs Traditional in impedance rendering

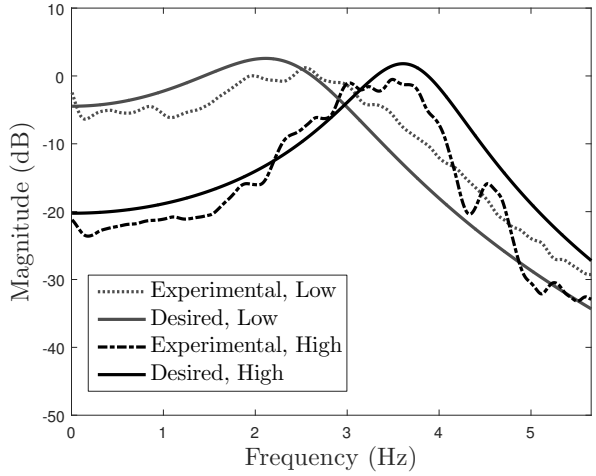

Fig. 12. Two different impedances rendered on SEA

REFERENCES

[1] N. Hogan, "Impedance Control: An Approach to Manipulation: Part IIImplementation," *J. Dyn. Sys., Meas., Control*, vol. 107, no. 1, pp. 8–16, 1985.

[2] D. E. Whitney, "Historical Perspective and State of the Art in Robot Force Control," *Int. J. of Robotics Research*, vol. 6, no. 1, pp. 3–14, 1987.

[3] R. Alami, *et al.*, "Safe and dependable physical human-robot interaction in anthropic domains" in *Intelligent Robots and Systems,IEEE/RSJ Int. Conf.*, 2006, pp. 1–16.

[4] S. Seok, *et al.*, "Actuator design for high force proprioceptive control in fast legged locomotion," in *Intelligent Robots and Systems,IEEE/RSJ Int. Conf.*, 2012, pp. 1970–1975.

[5] A. Albu-Schffer, C. Ott, and G. Hirzinger, "A unified passivity-based control framework for position, torque and impedance control of flexible joint robots,"*Int. J. of Robotics Research* vol. 26, no. 1, pp. 23–39, 2007.

[6] G. Pratt and M. Williamson, "Series elastic actuators," in *Intelligent Robots and Systems,IEEE/RSJ Int. Conf.*, 1995, pp. 399–406 vol.1.

[7] N. Paine, S. Oh, and L. Sentis, "Design and control considerations for high-performance series elastic actuators," *IEEE/ASME Trans. Mechatron.*, vol. 19, no. 3, pp. 1080–1091, 2014.

[8] N. Paine, *et al.*, "Actuator Control for the NASA-JSC Valkyrie Humanoid Robot," *J. Field Robotics*, vol. 32, no. 3, pp. 378–396, 2015.

[9] J. Lu, *et al.*, "Design and torque-mode control of a cable-driven rotary series elastic actuator for subject-robot interaction," in *Advanced Intelligent Mechatronics, IEEE Int. Conf.*, 2015, pp. 158–164.

[10] J. F. Veneman, *et al.*, "A Series Elastic- and Bowden-Cable-Based Actuation System for Use as Torque Actuator in Exoskeleton-Type Robots," *Int. J. of Robotics Research*, vol. 25, no. 3, pp. 261–281, 2006.

[11] C. Carignan, J. Tang, and S. Roderick, "Development of an exoskeleton haptic interface for virtual task training," in *IEEE/RSJ Int. Conf. Intelligent Robots and Systems*, 2009, pp. 3697–3702.

[12] L. M. Miller and J. Rosen, "Comparison of multi-sensor admittance control in joint space and task space for a seven degree of freedom upper limb exoskeleton," in *Biomedical Robotics and Biomechatronics, IEEE RAS and EMBS Int. Conf. on*, 2010, pp. 70–75.

[13] A. Nakai, *et al.*, "Arm type haptic human interface: Sensor arm," in *Proc. Int. Conf. Artificial Reality and Tele-Existence*, 1997, pp. 77–84.

[14] H. Kim, *et al.*, "Admittance control of an upper limb exoskeleton-Reduction of energy exchange," in *Eng. in Medicine and Biology Society, Annual Int. Conf.* 2012, pp. 6467–6470.

[15] T. H. Massie and J. K. Salisbury, "The phantom haptic interface: A device for probing virtual objects," in *Proc. of the ASME symposium on haptic interfaces for virtual environment and teleoperator systems*, vol. 55. 1994, pp. 295–300.

[16] H. I. Krebs, *et al.*, "Robot-aided neurorehabilitation," *IEEE Trans. Rehabil. Eng.*, vol. 6, no. 1, pp. 75–87, 1998.

[17] J. D. Chapel and R. Su, "Attaining impedance control objectives using H infinity design methods," in *Robotics and Automation, IEEE Int. Conf.*, 1991, pp. 1482–1487.

[18] M. J. Kim and W. K. Chung, "Design of nonlinear H optimal impedance controllers," in *Intelligent Robots and Systems, IEEE/RSJ Int. Conf.*, 2013, pp. 1972–1978.

[19] S. P. Buerger and N. Hogan, "Complementary stability and loop shaping for improved humanrobot interaction," *IEEE Trans. Robotics* vol. 23, no. 2, pp. 232–244, 2007.

[20] H. Mohammadi and H. Richter, "Robust tracking/impedance control: Application to prosthetics," in *American Control Conf.*, 2015, pp. 2673–2678.

[21] Z. Lu and A. A. Goldenberg, "Robust impedance control and force regulation: Theory and experiments," *Int. J. of Robotics Research*, vol. 14, no. 3, pp. 225–254, 1995.

[22] T. Murakami, *et al.*, "Force sensorless impedance control by disturbance observer," in *Power Conversion Conf., Conf. Record*, 1993, pp. 352–357.

[23] E. Sariyildiz and K. Ohnishi, "On the explicit robust force control via disturbance observer," *IEEE Trans. Ind. Electron.*,vol. 62, no. 3, pp. 1581–1589, 2015.

[24] N. Oda, *et al.*, "A robust impedance control strategy for redundant manipulator," in *Proc Int. Conf. Ind. Electronics, Control, and Instrumentation*, 1995, pp. 1254–1259 vol.2.

[25] R. Bickel and M. Tomizuka, "Disturbance observer based hybrid impedance control," in *Proc. American Control Conf.*, 1995, pp. 729–733 vol.1.

[26] S. H. Kang, M. Jin, and P. H. Chang, "A solution to the accuracy/robustness dilemma in impedance control," *IEEE/ASME Trans. Mechatron.*, vol. 14, no. 3, pp. 282–294, 2009.

[27] N. Colonnese and A. Okamura, "M-width: stability and accuracy of haptic rendering of virtual mass," *Robotics*, vol. 41, 2013.

[28] N. Hogan, "On the stability of manipulators performing contact tasks," *Robotics and Automation, IEEE J. of*, vol. 4, no. 6, pp. 677–686, 1988.

[29] D. A. Lawrence, "Impedance control stability properties in common implementations," in *Robotics and Automation, IEEE Int. Conf.*, 1988, pp. 1185–1190.

[30] K. Ohnishi, M. Shibata, and T. Murakami, "Motion control for advanced mechatronics," *IEEE/ASME Trans. Mechatron.* vol. 1, no. 1, pp. 56–67, 1996.

[31] B. D. O. Anderson, "The small-gain theorem, the passivity theorem and their equivalence," *J. of the Franklin Institute*, vol. 293, no. 2, pp. 105–115, 1972.

[32] K. Kong, J. Bae, and M. Tomizuka, "Control of rotary series elastic actuator for ideal force-mode actuation in humanrobot interaction applications," *IEEE/ASME Trans. Mechatron.*, vol. 14, no. 1, pp. 105–118, 2009.

[33] H. Vallery, *et al.*, "Passive and accurate torque control of series elastic actuators," in *Intelligent Robots and Systems, IEEE/RSJ Int. Conf.*, 2007, pp. 3534–3538.